

# Optical fibre long period grating gas sensor modified with metal organic framework thin films

Jiri Hromadka<sup>1,2</sup>, Begum Tokay<sup>3</sup>, Sergiy Korposh<sup>1,4</sup> and Stephen James<sup>4</sup>

<sup>1</sup>*Applied Optics Group, Electrical Systems and Optics Research Division, Faculty of Engineering, University of Nottingham, University Park, Nottingham NG7 2RD, United Kingdom*

<sup>2</sup>*Institute for Environmental Studies, Faculty of Sciences, Charles University in Prague, Benátská 2, CZ 12843 Praha 2, Czech Republic*

<sup>3</sup>*Chemical and Environmental Engineering Department, Faculty of Engineering, University of Nottingham, University Park, Nottingham NG7 2RD, United Kingdom*

<sup>4</sup>*Department of Engineering Photonics, School of Engineering, Cranfield University, Cranfield, Bedfordshire MK43 0AL, United Kingdom*

## Abstract

An optical fibre long period grating (LPG) modified with a thin film of ZIF-8, zeolitic imidazol framework material, a subgroup of metal organic framework (MOF) family, was employed for the detection of organic vapours. ZIF-8 film was deposited onto the surface of the LPG using in-situ crystallization technique by mixing freshly prepared 12.5 mM zinc nitrate hexahydrate and 25 mM of 2-methyl-imidazole solutions in methanol. ZIF-8 film was characterized by scanning electron microscope (SEM) images, thickness and refractive index (RI) has been calculated with use of ellipsometer for films containing of 1,2,3,5 and 10 growth cycles. The crystallinity of the film was confirmed by x-ray diffraction pattern (XRD). The LPG sensor was designed to operate at the phase matching turning point to provide the highest sensitivity. The sensing mechanism is based on the measurement of the RI change induced by the penetration of the chemical molecules into the ZIF-8 pores. LPG modified with 2 and 5 growth cycles of ZIF-8 responded to exposure to methanol, ethanol, 2-propanol and acetone. The sensitivity of the measurements to humidity as an interfering parameter was also investigated.

**Key words:** Long period grating (LPG), metal organic framework (MOF), zeolitic imidazol framework (ZIF), ZIF-8, organic vapour sensing

## 1. Introduction

Although the numerous chemical sensors already exist, there is still a place for new technologies. The new sensors could target the demand in areas of medical diagnostics food quality control, in air quality (occupational exposure) or in various fields of environmental monitoring [1]. Fabrication of low-cost, precise and real-time sensors for volatile organic compounds (VOCs) is in a high interest for VOCs detection as the GC-MS approach commonly used for total VOCs detection is expensive and needs experienced personnel [2]. The key element of any portable sensor is the sensitive layer that captures gases.

In this respect, metal organic frameworks (MOFs), because of their unique properties, offer an ideal platform for the development of the sensitive layer. They can be considered as

crystalline materials with tuneable porosity, large internal surface area and organic functionality. The strong metal-oxygen-carbon bonds imbue the materials with high chemical and thermal stabilities [3].

The various range of the possible applications of MOFs have been reviewed elsewhere [4], [5], [6] and main focus of their use is given to be selective hydrogen gas storage [7], selective gas adsorption [8], and separation [9] or catalysis [10].

The adjustment of the pore size and possible post-synthesis functionalization enable the specific reaction of selected type of MOF with analyte of interest where only certain molecules (treated by size or functional group) are allowed to enter into MOFs cavities. The initial research was based on the fabrication of different types of materials from MOF family however fabrication of these materials in the form of thin films is considered to be crucial for many applications especially for sensors and membranes [1] [11]. The fabrication of the films is challenging in the way to control the uniform cover over the substrate and possibly control over the thickness and growth direction of the crystals [11].

There have been limited reports of MOF based sensors, but they indicate their potential to become powerful analytical devices [1]. The main advantage is high chemical selectivity possible by the appropriate selection of the MOF with desired properties [5]. However, there is a need to establish a suitable means of signal transduction to enable the use of MOFs for chemical sensing [12]. The pores for all MOF structures are too small to incorporate reporting molecules. The most promising approach appears to be the adoption of macroscopic perspective and analyse changes in the properties of the whole film. This can be achieved by the use of optical transduction techniques, which require the fabrication of a film, ideally with controllable thickness, on an optical sensing platform such as a fibre optic long period grating (LPG).

Among the variety of MOFs, zeolitic imidazole framework (ZIF) - ZIF-8, possess properties that show promise for sensor development, such as its chemical robustness and thermal stability due to the sodalite (SOD) type of structure. The structure of ZIF-8 comprises zinc ions coordinated by four imidazolate rings with large cavities (11.6 Å) and small pore apertures (3.4 Å) [13]. ZIFs have been considered to behave as apolar adsorbents with molecular sieving properties. An investigation of a ZIF-8 film demonstrated the adsorption of isopropanol in a selective manner versus water [14]. A ZIF-8 based Fabry-Perot interferometer exhibited a concentration-specific reaction to a mixture of propane and nitrogen [12]. ZIF-8 film fabrication involves no substrate modification. The procedure works at room temperature and facilitates the control over the thickness with one growth cycle that takes less than an hour [12] [15].

The uniform ZIF-8 film fabrication involves no substrate modification. The procedure works at room temperature enables the control over the thickness with one deposition cycle that takes less than an hour [12] [15]. All of these factors were considered in the decision to follow this procedure and to deposit ZIF-8 thin film onto the surface of an optical fibre LPG.

Fibre-optic sensors have been considered as advantageous sensing platforms for the future as they are small, lightweight, immune to electromagnetic interference and as such can be used in extreme conditions, enabling remote real time monitoring with no electrical power needed at the sensing point [16]. Fibre-optic sensing platforms based on long period gratings (LPGs) with functional coatings have been used to measure various measurands including relative humidity [17], ammonia [18] and volatile organic compounds (VOCs) [19]. In addition, when the proteins, enzymes and antibodies are incorporated, then optical fibres can be used for biological response measurement [20].

An LPG consists of a periodic perturbation of the refractive index of the core of an, which couples the core mode to a set of co-propagating modes of the cladding of the fibre. This coupling is manifested in the transmission spectrum of the optical fibre as a series of loss, or

resonance bands. Each resonance band corresponds to coupling to a different cladding mode and each shows different sensitivity to environmental changes [21].

The coupling wavelength can be obtained from the following phase matching equation

$$\lambda_x = [n_{\text{core}} - n_{\text{clad}(x)}] \Lambda \quad (1)$$

Where  $\lambda_x$  represents the wavelength at which light is coupled to the  $LP_{0x}$  cladding mode,  $n_{\text{core}}$  is the effective refractive index of the mode propagating in the core of the fibre,  $n_{\text{clad}(x)}$  is the effective index of the  $LP_{0x}$  cladding mode and  $\Lambda$  is the period of the LPG [21]. The central wavelength of the resonance band is sensitive to changes in environmental conditions such as strain, temperature, bending radius and refractive index of the surrounding conditions [18] [21]. Fibre-optic sensing platforms based on long period gratings (LPGs) with functional coatings have been used to measure various measurands including relative humidity [17], ammonia [18] and volatile organic compounds (VOCs) [19]. In addition, when the proteins, enzymes and antibodies are incorporated, then optical fibres can be used for biological measurement [20].

It has been shown that the phase matching condition for each cladding mode contains a turning point and that the LPG exhibits the highest sensitivity when phase matching turning point (PMTP) is reached that can be achieved by choosing an appropriate LPG period and coating thickness [19] [22].

In this work, we fabricated LPG based chemical vapour sensor, which uses ZIF-8 as a functional coating of optical fibre LPG. ZIF-8 film was characterized by scanning electron microscope (SEM) images, thickness and refractive index (RI) has been calculated with use of ellipsometer for films containing of 1,2,3,5 and 10 growth cycles. The crystallinity of the film was confirmed by x-ray diffraction pattern (XRD). The LPG coated with ZIF-8 thin film was exposed to methanol, ethanol, 2-propanol and acetone vapours, where the concentration specific response to methanol was shown and the limit of detection (LOD) was calculated. The response to water, a potential interfering measurand, was also investigated.

## 2. Experiment

### 2.1 Materials

Zinc nitrate hexahydrate, 2-methyl-imidazole, methanol, ethanol, 2-propanol and acetone were purchased from Sigma-Aldrich. All of the chemicals were analytical grade reagents and used without further purification.

### 2.2 Characterization of ZIF-8 film

#### 2.2.1 Characterizations of film structures

Scanning electron microscopy (SEM) was used to evaluate the structure and the thickness of the films deposited on glass substrates. Measurements were undertaken by Philips XL30 FEG ESEM electron microscope with 10 kV beam voltage. Glass slides about  $1 \times 1 \text{ cm}^2$  and  $2 \times 2 \text{ cm}^2$  were cut from standard microscope glass slides and then coated with ZIF-8 thin film following procedure described in section 2.2. Samples containing 1,2,3,5 and 10 growth cycles of ZIF-8 were characterized by SEM.

Thin Pt layers were sputtered on all samples before the SEM analysis. The sputter was set to of 0.8kV voltage and 0.7mA current. Glass slides were sputtered by two layers of the Pt coating with deposition interval of 90 seconds.

### 2.2.2 Ellipsometry measurements

A thickness of the films has been further evaluated on glass substrates with use of an ellipsometer. The measurements were undertaken by Alpha-SE Ellipsometer (J.A Woolan) with use of model considering transparent film on a glass substrate and with 10 s data acquisition rate. Data were collected at a spectral resolution of 1 nm and measured in the wavelength range of 380–900 nm; for simplicity the RI value of the mesoporous film was determined at one wavelength (632.8 nm).

### 2.2.3 Crystallographic analysis

The x-ray diffraction patterns were collected using a Bruker-AXS D8 Advance diffractometer, using  $\theta/\theta$  goniometer geometry, a Cu-anode line-focus x-ray tube (powered at 40 kV & 35 mA), a Göbel mirror (producing a parallel  $\text{CuK}\alpha$  beam) with a 0.6 mm exit slit, a diffracted beam  $0.12^\circ$  Soller-slit collimator and a scintillation counter x-ray detector. The samples were scanned with a fixed glancing incident angle of  $2.140$  and  $1.140^\circ$ , over a  $2\theta$  range of  $5^\circ$  to  $40^\circ$ , with a  $2\theta$  step size of  $0.02^\circ$  and a step time of 32 s.

## 2.2 Sensor fabrication

LPGs with grating periods of  $110.7 \mu\text{m}$  of length 40 mm, was fabricated in boron–germanium co-doped optical fibre (Fibercore PS750) with cut-off wavelength 670 nm in a point-by-point fashion, side-illuminating the optical fibre by the output from a frequency-quadrupled Nd:YAG laser, operating at 266 nm [23].

The transmission spectrum of the optical fibre was recorded by coupling the output from a tungsten-halogen lamp (Ocean Optics HL-2000) into the fibre, analysing the transmitted light using a fibre coupled CCD spectrometer (Ocean Optics HR4000), Figure 1. The grating period was selected such that the LPG operated at or near the phase matching turning point [19] [22], which, for coupling to a particular cladding mode (in this case  $\text{LP}_{019}$ ), ensured optimized sensitivity.

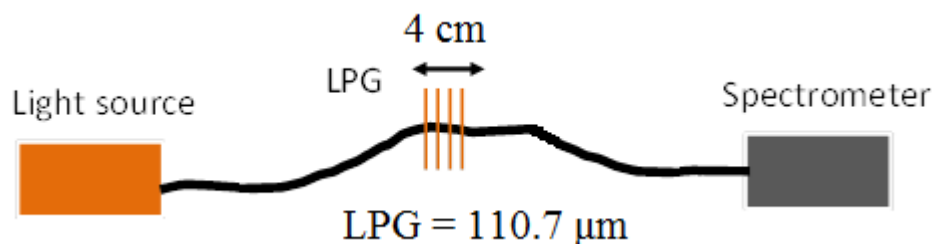


Figure 1: Schematic illustration of the LPG sensor

LPG was coated with ZIF-8 by in situ crystallization technique, Figure 2 [12] [15]. Briefly, solutions of 15 ml of 12.5 mM zinc nitrate hexahydrate and 15 ml of 25 mM 2-methylimidazole in methanol were mixed in a Petri dish. The LPG was fixed in a specially designed holder to keep LPG tight and straight. The LPG was placed inside the Petri dish and immersed into film forming solution for a period of 30 min. Then LPG sensor was washed by methanol and dried under nitrogen flow. The process was repeated to obtain thicker films consisting of 2 and 5 growth cycles.

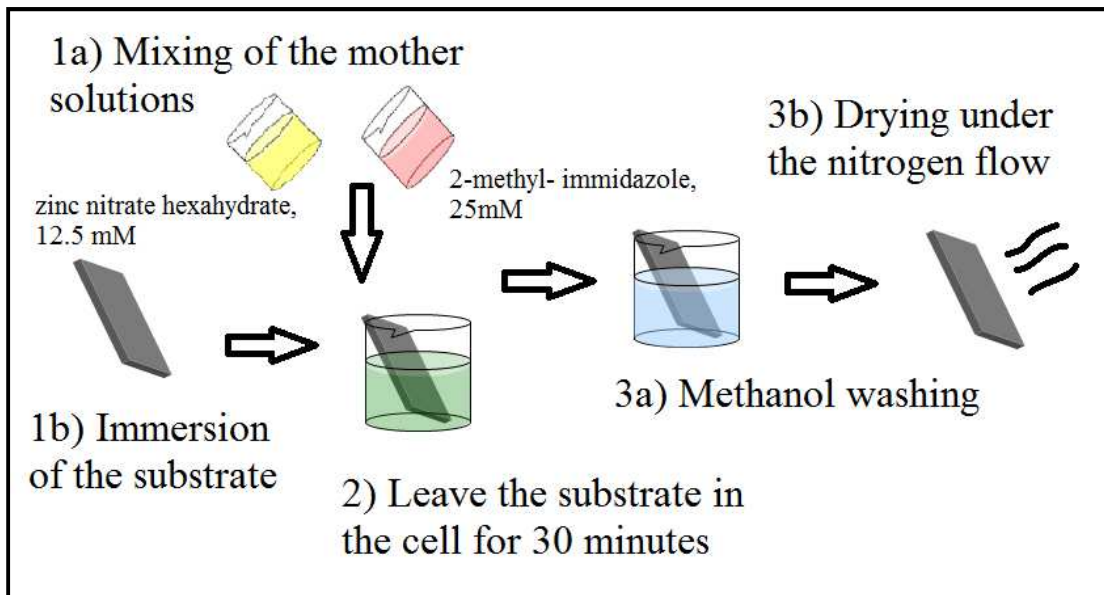


Figure 2: ZIF-8 fabrication methodology [12]

The transmission spectra of the LPG were measured during the each deposition step with acquisition interval of 10 seconds.

### 2.3 Sensor performance

Performance of the LPG as a chemical sensor was investigated by exposing the sensor to methanol, ethanol, 2-propanol and acetone vapours. VOCs samples of volume of 200  $\mu$ l were injected by pipette into a container containing the LPG (Figure 3). The transmission spectra were monitored with acquisition interval of 10 seconds. Water droplet was also injected for comparison reasons to identify the response to relative humidity, a potential interfering factor.

The position of the central wavelength has been monitored and its shift corresponding to the presence of chemical vapour was evaluated.

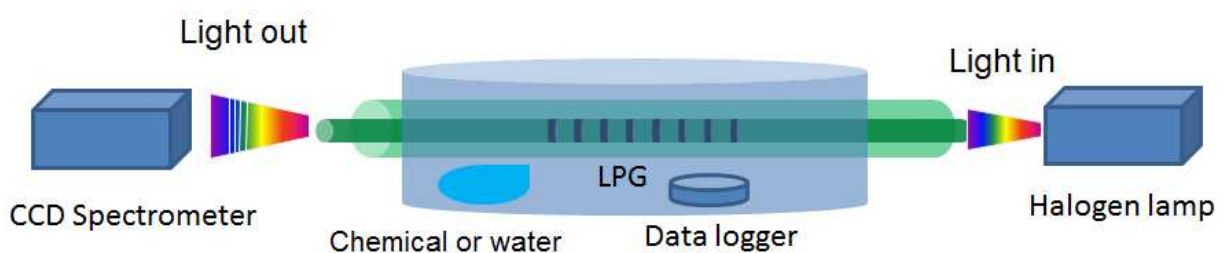


Figure 3: Experimental set-up for chemical sensitivity experiments.

Methanol calibration test had been conducted in an environmental chamber, which is composed of closed polytetrafluoroethylene (PTFE) box (15x15x15 cm). The LPG was placed inside the box in a fixed position about 5 cm above the base. Methanol (10 or 50  $\mu$ l) was injected from the top of the box by pipette and the transmission spectrum was simultaneously monitored and recorded. The concentration was calculated according to the amount of methanol injected and the volume of the box.

Temperature and relative humidity (RH) were also recorded during all experiments with logging interval of 10 seconds by data logger (iButton® Hygrochron Temperature/Humidity

Logger, part number DS1923, from Maxim Integrated™ with precision of +/-0.5 °C and +/-0.6 RH %).

### 3. Results and discussion

Begum suggested to start with the film characterization as it is presented, Sergiy suggested to change structure slightly – please let me know

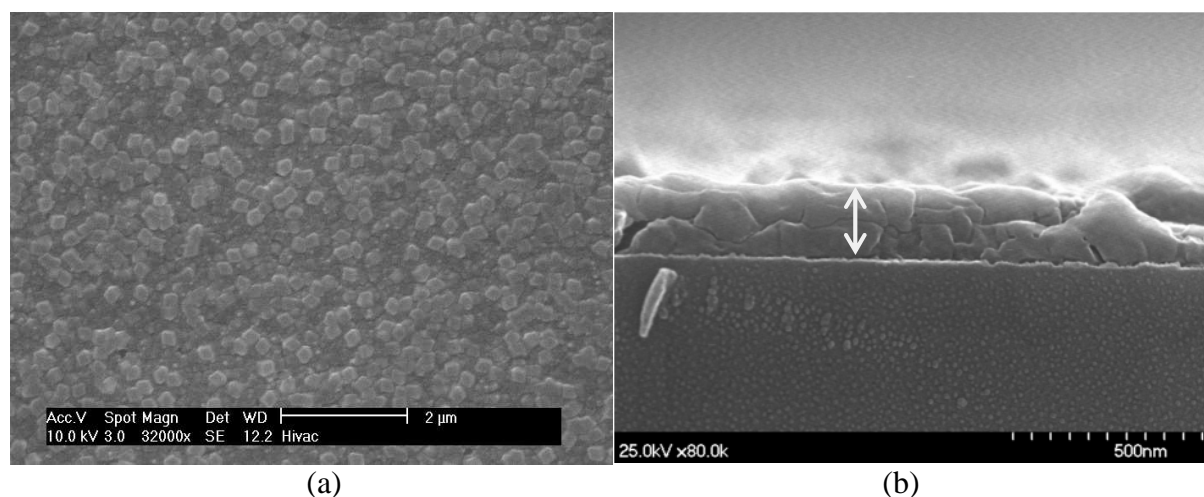
1. Describe first LPG behavior. Get as much as possible out of it, shift /cycle, optical thickens calculation, real time observations (was this done before if yes, how this corresponds to what was published before).
2. SEM, ellipsometer and XRD to support what you have stated with LPG.
3. VOCs measurements
  - Response dynamic and TS (calculate response time)
  - Thickness dependence
  - Calibration curves (calculate limit of detection)

#### 3.1 Film morphology

SEM images show the uniform cover over the substrate as well as the uniformity over the thickness of the deposited ZIF-8 film, Figure 4a. The density of the crystals over the substrates is affected by the concentration of the film forming solution, while the selected one (12.5 mM for Zn source and 25 mM from methyl-imidazole) has been realized as optimal [15].

The horizontal size of the crystals in the ZIF-8 film was observed to increase as a function of growth cycle, starting at approximately 100 nm and end with size of about 400 nm in a film containing 1 and 10 growth cycles respectively. This effect was observed through substrates coated with 1, 3, 5 and 10 growth cycles (Figure S1) and it could be denoted by the agglomeration of the freshly crystalized ZIF-8 units onto the surface of the existing ones, in a similar way as it was described for the seeded growth fabrication technique [11]. The increase of the crystal sizes with increasing number of growth cycles has been observed before for substrates comprised of 1, 10 and 40 growth cycles [12].

The film thickness has been evaluated with use of cross-sectional SEM imaging and film with 10 growth cycles indicates the thickness of about 400 nm, Figure 4b, which is approximately about half of the level presented earlier with use of the same deposition method [12]. This could well be due to the differences in the nitrogen flow rate or the exact vertical position of substrates in the Petri dish during the crystallization process in the film forming solution.



(a)

(b)

Figure 4: a) Top view and b) cross sectional SEM images of ZIF-8 films grown on glass substrates with 5 and 10 growth cycles respectively

Ellipsometry measurements had been conducted to investigate the thickness of the substrates coated with 1,2,3,5 and 10 growth cycles. A linear dependence of the MOFs film thickness on number of the deposited cycles was obtained with the slope of approximately 50 nm per growth cycle, Figure 5. These results correspond well with the data obtained using SEM images (in Figure 4b).

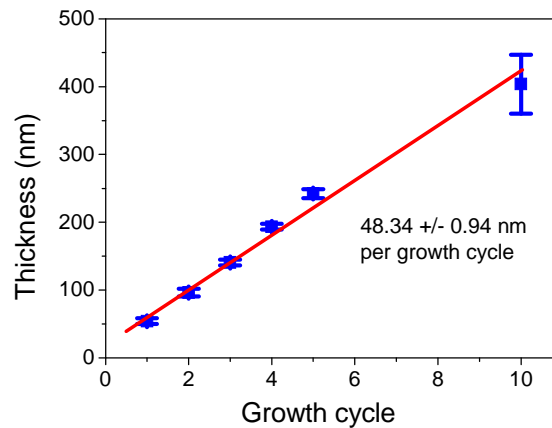


Figure 5: Ellipsometry measurement: thickness of ZIF-8 film as a function of growth cycle (average value is shown and error bars were calculated as the standard deviation from the measurement over the 3 substrates)

Refractive index (RI) was measured by ellipsometry and a nonlinear relation between growth cycle and RI was observed. RI values varied from 1.48 to 1.40 for a film composed of 1 and 10 growth cycles respectively. Interestingly, this change corresponds to the size of the crystals (Figure S1). Larger crystals were observed on the substrates at the higher number of growth cycles which could denote presence of larger mesopores in the film structure [24]. Refractive index of ZIF-8 films strongly depends on the selected crystallization method and conditions during fabrication. The big variations in RI values were published. Demessence et al reported ZIF-8 films with RI ranging from 1.18 and 1.23 [14]. On the other hand, Cookney et al obtained ZIF-8 films with much higher RI ranging from 1.54 to 1.58, which was related to the low porosity these films [24].

### 3.2. Film structure

X-ray diffraction patterns establish that the films comprise ZIF-8 crystals, Figure 6. The positions of the peaks (110), (200), (211), (220), (310) and (322) indicate crystalline ZIF-8 structure. The highest intensity at (110) reflection peak suggests the orientation of the film perpendicular to the substrate. The elevated plateau from 15 to 40  $\theta^\circ$  relates to the amorphous structure of the glass substrate. The position and the intensity of the peaks in Figure 6 are in a good agreement with the X-ray diffraction patterns presented in the literature and as well with the modelled diffraction pattern for ZIF-8 [12] [25].

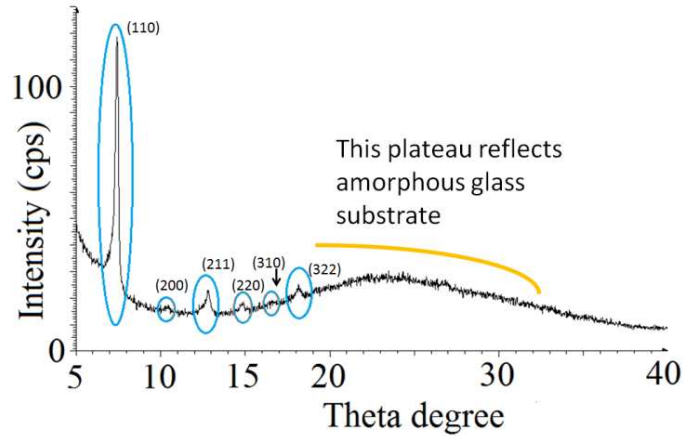


Figure 6: In-plane X-Ray diffraction patterns of ZIF-8 film grown on glass substrate via 20 growth cycles, recorded at room temperature

### 3.3.LPG coating

The transmission spectrum of unmodified LPG with period of 110.7  $\mu\text{m}$  is shown in Figure 7. Attenuation bands in the region of 775 and 900 nm correspond to the  $\text{LP}_{019}$  cladding mode and operate at the PMTP while the other ones (region of 625 and 670 nm) correspond to lower cladding modes and are less sensitive for this LPG period.

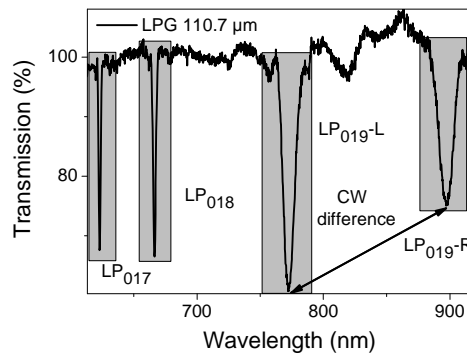


Figure 7: Transmission spectrum of the bare LPG with period of 110.7 $\mu\text{m}$  measured in air with attenuation bands (grey frames) corresponding to the  $\text{LP}_{018}$  and  $\text{LP}_{019}$  cladding modes (the dual resonance was observed for the  $\text{LP}_{019}$  cladding mode).

The changes in the transmission spectra in the film forming solution have been observed, where the transmission spectra after 30 min of immersion were compared, Figure S2a. The shift of the,  $\text{LP}_{019}$ -L,  $\text{LP}_{019}$ -R and  $\text{LP}_{018}$  central wavelengths in the film forming solution over the 1<sup>st</sup> to 5<sup>th</sup> growth cycle deposition ranged from 2.26 to 2.77 nm and with an average of  $2.58 \pm 0.24$  nm,  $3.50 \pm 1.40$  nm and  $0.58 \pm 0.13$  nm, respectively (the error bars are higher as they were calculated as the standard deviation of a sample containing only 4 values). The bigger shift of the central wavelength was observed in the solution than in air and it denotes to the higher refractive index of the film forming solution. (The central wavelength position reacts on the changes in optical thickness that relates to RI.)

The bigger shift of the central wavelength during the deposition was observed for  $\text{LP}_{019}$ -R, where the higher sensitivity in comparison to  $\text{LP}_{019}$ -L can be explained by the different slope of the phase matching curves before and after the reaching the PMTP [22] [19].

The growing separation of the attenuation bands corresponding to  $\text{LP}_{019}$ -L and  $\text{LP}_{019}$ -R can

be expressed as the change of the difference between the central wavelengths, where this change ranged from 150.61 to 174.19 nm, with the smallest shift in difference of 4.28 nm was observed at the end of immersion of the first growth cycle and with the average shift of  $5.90 \pm 1.29$  nm.

The change in transmission spectra of all attenuation bands was observed in air after the deposition of each of 1<sup>st</sup> to 5<sup>th</sup> growth cycle of ZIF-8, Figure 8a.

The shift in the difference between the central wavelengths corresponding to the LP<sub>019</sub> cladding mode and the shift of the central wavelength corresponding to the LP<sub>018</sub> and LP<sub>019</sub>-L and LP<sub>019</sub>-R cladding mode have been compared to show the higher sensitivity of the sensor operating close to the PMTP, Figure 8b. The change of the central wavelengths difference in air after the deposition of 1<sup>st</sup> to 5<sup>th</sup> growth cycle ranged from 1.99 to 4.23 nm, with an average of  $3.33 \pm 0.84$  nm. Similarly to the values measured in solution, the smallest value was obtained for the first growth cycle. For comparison, the central wavelength shift corresponding to LP<sub>018</sub> cladding mode range from 0.25 to 0.51 nm with an average of  $0.36 \pm 0.14$  nm. We can conclude the linear dependence between a number of growth cycles and the shift in the central wavelength difference, Figure S3.

Smaller value for the first growth cycle could correspond to the difficulty for the crystals to attach the surface of the bare LPG. The smaller thickness of the film after the first deposited growth cycle was presented by Lu and Hupp with use of silica substrates [12].

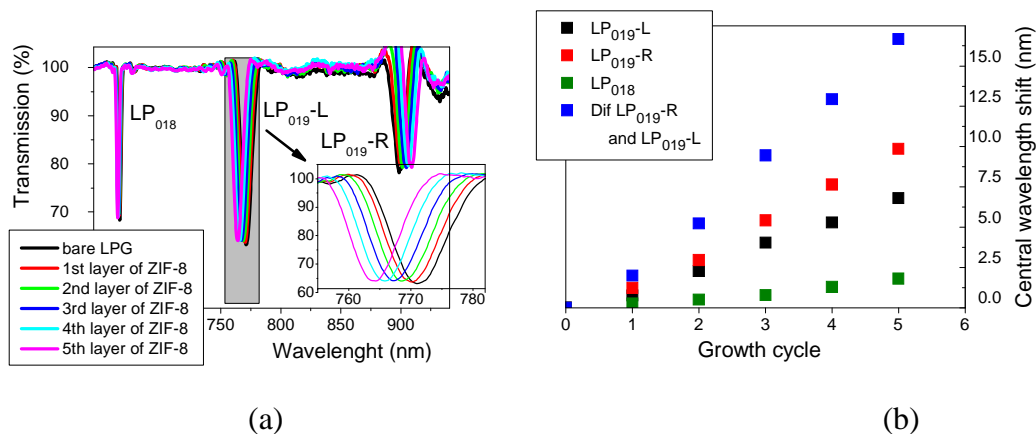


Figure 8: a) transmission spectra of the LPG measured in air; black line, bare LPG and after the deposition of 1<sup>st</sup> to 5<sup>th</sup> growth cycle of ZIF-8; red, green blue, cyan and magenta lines and b) change in the position of the central wavelength corresponding to LP<sub>018</sub>, LP<sub>019</sub>-L, LP<sub>019</sub>-R cladding modes and the change in the difference between the central wavelengths corresponding to LP<sub>019</sub> cladding mode (blue) during the deposition of 1<sup>st</sup> to 5<sup>th</sup> growth cycle of ZIF-8

The linear dependency between the shift of the difference between the central wavelengths and the number of growth cycles correlates very well with the thickness measurement taken by the ellipsometer. The change in the central wavelength difference can be expressed as a function of the optical thickness, that can be calculated as a product of RI and thickness of the ZIF-8 film (both values were obtained from the ellipsometer and are shown in Section 3.1). The shift in the difference between the central wavelengths of 5 nm corresponds to the change of optical thickness of 100 nm and the linear dependency between both variables was obtained, Figure 9.

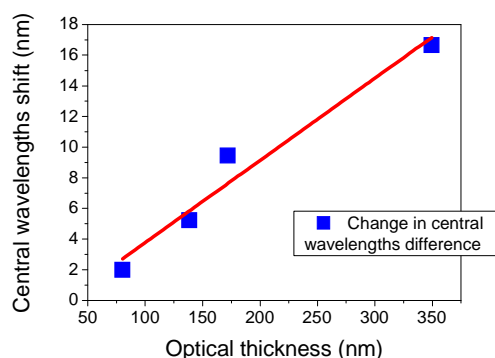


Figure 9: The change in the separation of central wavelengths corresponding to  $LP_{019}$  cladding mode induced by the deposition of ZIF-8 as a function of optical thickness

The transmission spectra during the whole deposition process have been recorded and the dynamic change in the separation between the  $LP_{019-L}$  and  $LP_{019-R}$  bands is shown in Figure 10a. There is possible to identify two regions of values, first slightly increasing from  $\sim 127$  to  $\sim 140$  nm corresponds to the transmission spectra taken in air and the second, from  $\sim 150$  to  $\sim 175$  nm corresponds to the time while LPG was immersed in the film forming solution (the immediate change is caused by a higher RI of the solution, the continuous change after denotes to the crystallization of ZIF-8 onto the surface of LPG).

The oscillation of the central wavelength occurring after the immersion process is due to the nitrogen flow that affects the spectra in two ways. Firstly, the central wavelength change is caused only by the mechanical response of the LPG to the flow which causes slight movement and bending and secondly, the chemical process is taking a place in the freshly crystallized ZIF-8 film, where methanol is being replaced by nitrogen and then subsequently replaced by air in the ZIF-8 pores until the final crystalline ZIF-8 structure is reached on the surface of LPG.

The rapid decrease of the central wavelength occurring immediately after the immersion in the film forming solution indicates that the crystallization process starts rapidly and a high efficiency was observed within the first 10 minutes. Evolution of the transmission spectrum while the LPG was immersed in the film forming solution (for the 1<sup>st</sup> growth cycle, labelled as the grey box in Figure 10a), shown in Figure S2b at selected time intervals for  $LP_{019-L}$  attenuation band, were used for the evaluation of the film fabrication process, Figure 10b.

The change in the difference between central wavelengths in time gives the opportunity to observe the efficiency of the crystallization during the deposition in real time. It is possible to identify that the crystallization process starts rapidly, with a 50 % and 90 % of the central wavelength change reached within  $\sim 5$  and  $\sim 20$  min respectively.

This finding is in a good agreement with real time measurement during the film deposition reported with use of Quartz Crystal Microbalance (QCM) measurement of ZIF-8 film growth where changes in frequency and mass were measured for 2 hours and the 90 % mass change taken a place within 30 minutes and for this reason authors decided to set the growth cycle immersion for 30 min. When only the data from the first 30 min are compared, then reaching the 50 % crystallization efficiency within  $\sim 5$  min after the immersion can be concluded [12].

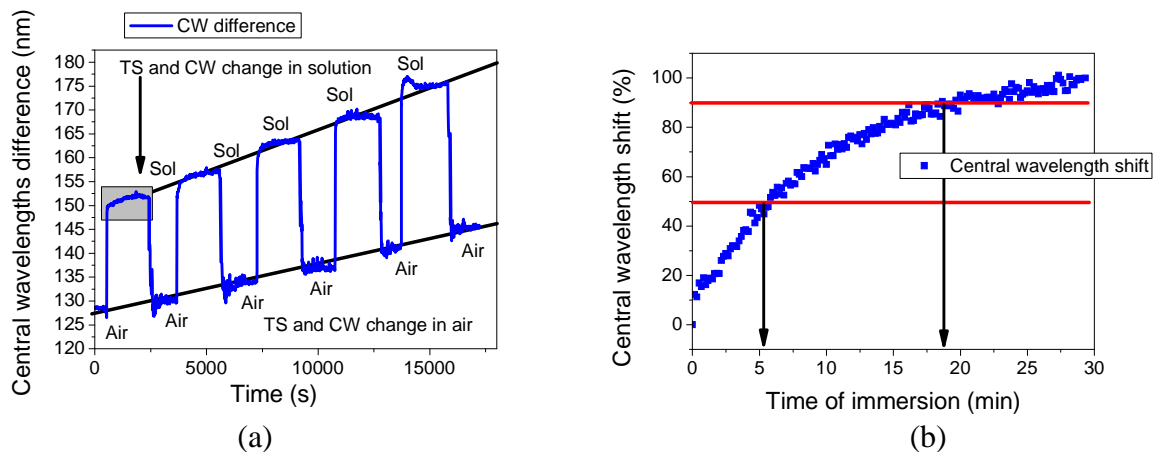


Figure 10: The dynamic shift of the central wavelength during the deposition of 1<sup>st</sup> to 5<sup>th</sup> growth cycle onto a surface of LPG and b) relative shift of the central wavelength during the immersion in the film forming solution over the deposition of 1<sup>st</sup> growth cycle

### 3.4 VOCs sensing

The immediate response (less than 30 s) of the LPG transmission spectrum was observed after the placement of all the tested VOCs to the proximity of the sensor while the maximum shift of the central wavelength was reached in less than one minute for methanol and acetone and about three minutes for ethanol and 2-propanol. The response time correlates with differences in volatility, where the highest value is expected for acetone, then methanol, ethanol and 2-propanol, respectively. (Evaporation rate is affected by the functional group, partial pressure of the saturated vapour, molecular weight, surface of the spill and air flow over the spill.)

The highest response of the sensor was observed for methanol, where the change in the bands separation due to the concentrated vapours about 4.23 nm was obtained in comparison to 2.4 nm shift induced by ethanol for the sensor coated by 5 growth cycles, Figure 11a. The inset is showing the LP<sub>019</sub>-L attenuation band in detail, where the central wavelength shift of 2.7 and 1 nm was observed for methanol and ethanol, respectively. Similarly, the transmission spectra are shown for acetone and 2-propanol, where the maximal change in the band separation reached 3.64 and 2.65 nm, respectively Figure S4.

Amplitude change of the LP<sub>019</sub>-L band was observed with decrease of the transmission loss due to the chemical vapours. Similar to the central wavelength, the highest intensity change was observed for methanol, while the level of transmission increased from 62.53% measured in air to 64.51 and 66.70% measured when LPG was exposed to ethanol and methanol vapours, respectively (the transmission values were taken at time when the maximum shift of the central wavelength was reached).

Similarly the highest response to methanol was observed for the sensor coated with 2 growth cycles of ZIF-8, Figure 11b. The change in band separation was measured of 4.12, 5.09 and 3.79 nm for methanol and the shift corresponding to 0.72, 0.83 and 3.64 nm was induced by ethanol, 2-propanol and acetone, respectively. In comparison, the shift of the central wavelength corresponding to LP<sub>018</sub> cladding mode reached only 1.75, 2.03 and 1.98 for methanol and 0.45, 0.45 and 1.77 nm for ethanol, 2-propanol and acetone. The minimal response was observed for water (central wavelength shift of 0.4 (band separation of LP<sub>018</sub>) and 0.2 nm (central wavelength shift of LP<sub>018</sub>) corresponding to relative humidity increase from  $\approx 40$  to  $\approx 70$  %).

The sensors show perfect reversibility as the transmission spectra returned to their initial positions within the 10 minutes after the maximum shift of the central wavelength was

observed. The differences between the recovery times of the individual VOCs tested were corresponding to the differences in volatility in a same way as for the response time (the response time less than 3 minutes was observed for acetone, about 5 minutes for methanol and about 10 minutes for 2-propanol and ethanol), Figure 11b.

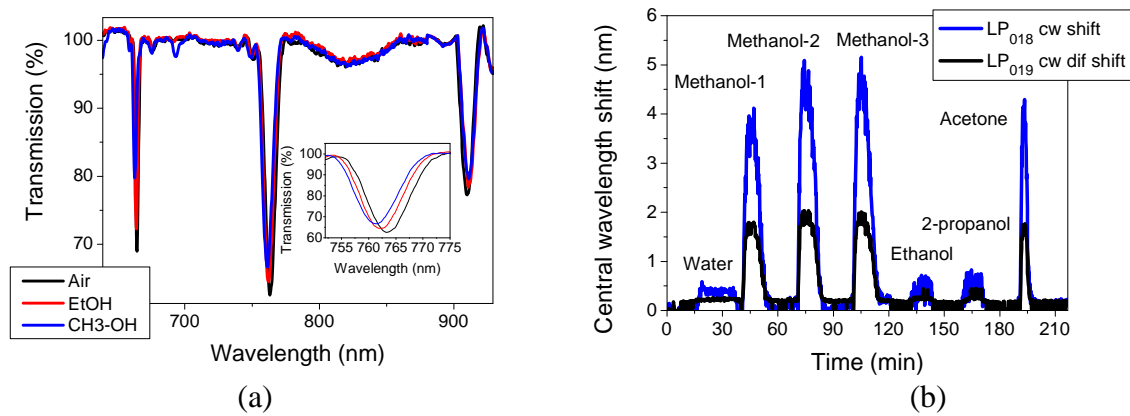


Figure 11: Transmission spectra of the LPG sensor with 5 growth cycles of ZIF-8 film exposed to methanol (blue) and ethanol (red) and b) dynamic shift of the shift of the central wavelength corresponding to LP<sub>018</sub> cladding mode (black) and the shift in the difference of the central wavelengths corresponding to LP<sub>019</sub> cladding mode (blue) of the LPG sensor coated with 2 growth cycles of ZIF-8 as the response to different organic vapours and water (for comparison)

The experiments in the open system showed the response of the LPG to different organic vapours however they don't enable to compare properly the effect of the number of growth cycles (thickness) on the sensitivity and don't enable to show concentration specific response and calibration. Methanol, for its highest response in the previous experiments, was chosen to examine the response of the sensor over the various range of concentration. The effect of the thickness of the film on the sensitivity was also investigated, while higher sensitivity was observed for the sensor coated with 5 growth cycles. The changes in the central wavelengths difference of 2.17 nm and 1.52 nm were measured for methanol concentration of 9,000 ppm for the sensor coated by 5 and 2 growth cycles, respectively. Minimal change in intensity at the central wavelength was observed, where transmission increase from 70.12 to 71.35%. The attenuation band shift of the sensor coated with 5 growth cycles is shown in Figure 12a.

The sensor coated with 5 growth cycles was exposed to methanol concentrations ranged from 1,790 to 27,900 ppm, the central wavelength shift was measured and the calibration curve calculated, where the logistic function appeared to be the most appropriate, Figure 12b. Similar experiment had been conducted for the sensor coated with 2 growth cycles however no further shift has been shown for concentrations over 9,000 ppm, Figure S5.

The limit of detection (LOD) of 1454 ppm was calculated for the sensor coated with 5 growth cycles, while this concentration was taken from the calibration curve in Figure 12b and corresponds to 0.065 nm shift of central wavelength, the half of the resolution of the spectrometer.

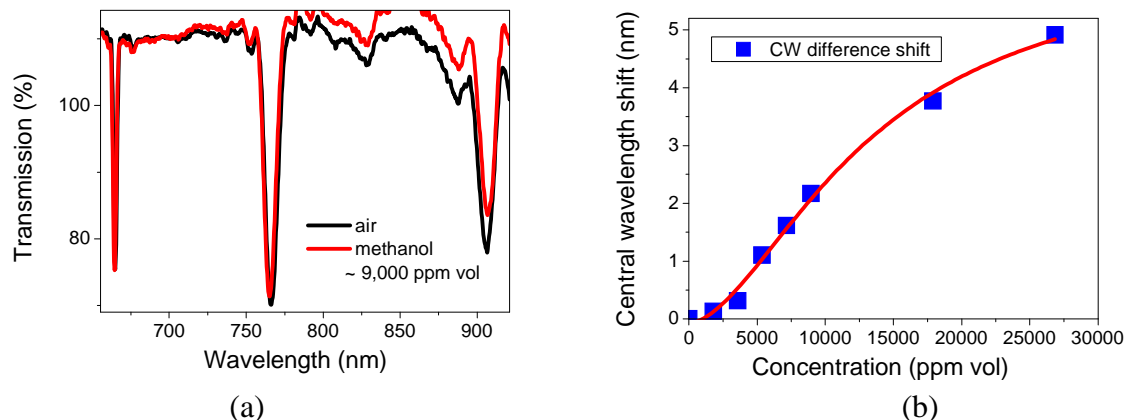


Figure 12: LPG sensor with 5 growth cycles of ZIF-8: a) shift in transmission spectrum corresponding to approximately 9,000 ppm of methanol and b) methanol calibration curve

#### 4. Conclusions

ZIF-8 film with a controllable thickness has been successfully deposited onto the surface of the optical fibre LPG with period of  $110.7 \mu\text{m}$  and the response of the transmission spectra has been characterized. X-ray diffraction patterns proved the desired crystal structure of the film and the ellipsometry measurements showed the direct proportion between the crystallization growth cycle and the film thickness corresponding approximately to a slope of  $50 \text{ nm}$  per growth cycle. The change in the transmission spectra expressed by the shift of the central wavelength has been shown as the function of the optical thickness of ZIF-8 film deposited onto the surface of LPG.

The LPG coated with 2 and 5 growth cycles of ZIF-8 showed the chemical sensitivity to methanol, ethanol, 2-propanol and acetone vapours. The response of the sensor has been measured in air. The response of the sensor was examined by the shift the central wavelength and highest sensitivity was observed for methanol that could be denoted due to use of methanol in film forming solution and then the size of the pores refers to the size of the methanol molecule.

The immediate response of the sensor was observed with a measurement of maximum response and recovery time less than three and ten minutes respectively however these values were affected by different volatility of the analytes in the open system.

The concentration specific response has been shown for methanol vapours for sensor coated with 2 and 5 growth cycles. Higher sensitivity was observed for the sensor coated with 5 growth cycles which indicates higher sensitivity with increasing thickness however issues with the intensity change, decrease of the transmittance loose of the attenuation band of LPG, can be expected with increasing film thickness. The limit of detection was stated to  $1454 \text{ ppm}$  for a sensor with non-optimized sensitivity.

Further work will include the chemical sensing and optimization of the (optical) thickness of the film, the investigation of the cross sensitivity of the material, identifying and deposition of the other materials from MOF family on the surface of LPG or fabrication of other types of fibre optic sensors, all of that with a target of development sensors with high selectivity and sensitivity.

#### ADD Acknowledgements

## References

- [1] L. Kreno, K. Leong, O. Farha, M. Allendorf, R. Van Duyne and J. Hupp, "Metal-organic framework materials as chemical sensors," *Chemical Reviews*, vol. 112, no. 2, pp. 1105-1125, 2012.
- [2] T. Nathanson, "Indoor air quality in office buildings: A technical guide," Federal-Provincial Advisory Committee on Environmental and Occupational Health, Minister of National Health and Welfare, 1995.
- [3] O. Yaghi, M. O'Keeffe, N. Ockwig, H. Chae, M. Eddaoudi and J. Kim, "Reticular synthesis and the design of new materials," *Nature*, vol. 423, no. 6941, pp. 705-714, 2003.
- [4] H. Furukawa, K. Cordova, M. O'Keeffe and O. Yaghi, "The chemistry and applications of metal-organic frameworks," *Science*, vol. 341, no. 6149, p. paperd ID 1230444, 2013.
- [5] R. Kuppler, D. Timmons, Q.-R. Fang, J.-R. Li, T. A. Makal, M. D. Young, D. Yuana, D. Zhao and W. Z. H.-C. Zhuang, "Potential applications of metal-organic frameworks," *Coordination Chemistry Reviews*, vol. 253, no. 23-24, pp. 3042-3066, 2009.
- [6] U. Mueller, M. Schubert, F. Teich, H. Puetter, K. Schierle-Arndt and J. Pastré, "Metal-organic frameworks—prospective industrial applications," *Journal of Materials Chemistry*, vol. 16, no. 7, pp. 626-636, 2006.
- [7] M. Suh, H. Park, T. Prasad and D.-W. Lim, "Hydrogen storage in metal-organic frameworks," *Chemical Reviews*, vol. 112, no. 2, pp. 782-835, 2012.
- [8] J.-R. Li, J. Sculley and H.-C. Zhou, "Metal-organic frameworks for separations," *Chemical Reviews*, vol. 112, no. 2, pp. 869-932, 2012.
- [9] J.-R. Li, R. Kuppler and H.-C. Zhou, "Selective gas adsorption and separation in metal-organic frameworks," *Chemical Society Reviews*, vol. 38, no. 5, pp. 1477-1504, 2009.
- [10] M. Yoon, R. Srirambalaji and K. Kim, "Homochiral metal-organic frameworks for asymmetric heterogeneous catalysis," *Chemical Reviews*, vol. 112, no. 2, pp. 1196-1231, 2012.
- [11] A. Bétard and R. Fischer, "Metal-organic framework thin films: From fundamentals to applications," *Chemical Reviews*, vol. 112, no. 2, pp. 1055-1083, 2012.
- [12] G. Lu and J. Hupp, "Metal-organic frameworks as sensors: A ZIF-8 based fabry-pérot device as a selective sensor for chemical vapors and gases," *Journal of the American Chemical Society*, vol. 132, no. 23, pp. 7832-7833, 2010.
- [13] K. Park, Z. Ni, A. Côté, J. Choi, R. Huang, F. Uribe-Romo, H. Chae, M. O'Keeffe and O. Yaghi, "Exceptional chemical and thermal stability of zeolitic imidazolate frameworks," *Proceedings of the National Academy of Sciences of the United States of America*, vol. 103, no. 27, pp. 10186-10191, 2006.
- [14] A. Demessence, C. Boissière, D. Grosso, P. Horcajada, C. Serre, G. Férey, G. Soler-Illia and C. Sanchez, "Adsorption properties in high optical quality nanoZIF-8 thin films with tunable thickness," *Journal of Materials Chemistry*, vol. 20, no. 36, pp. 7676-7681, 2010.
- [15] G. Lu, O. Farha, W. Zhang, F. Huo and J. Hupp, "Engineering ZIF-8 thin films for hybrid MOF-based devices," *Advanced Materials*, vol. 24, no. 29, pp. 3970-3974, 2012.
- [16] A. Kersey, "A review of recent developments in fiber optic sensor technology," *Optical Fiber Technology*, vol. 2, no. 3, pp. 291-317, 1996.

- [17] T. Venogupalan, T. Sun and K. T. V. Grattan, "Long period grating-based humidity sensor for potential structural health monitoring," *Sensors and Actuators, A: Physical*, vol. 148, no. 1, pp. 57-62, 2008.
- [18] S. Korposh, R. Selyanchyn, W. Yasukochi, S.-W. Lee, S. James and R. Tatam, "Optical fibre long period grating with a nanoporous coating formed from silica nanoparticles for ammonia sensing in water," *Materials Chemistry and Physics*, vol. 173, pp. 784-792, 2012.
- [19] S. Topliss, S. James, F. Davis, S. Higson and R. Tatam, "Optical fibre long period grating based selective vapour sensing of volatile organic compounds," *Sensors and Actuators, B: Chemical*, vol. 143, no. 2, pp. 629-634, 2010.
- [20] F. Arregui, I. Matias, J. Corres, I. Del Villar, J. Goicoechea, C. R. Zamarrenoa, M. Hernandez and R. Claus, "Optical fiber sensors based on layer-by-layer nanostructured films," *Procedia Engineering*, vol. 5, pp. 1087-1090, 2010.
- [21] S. James and R. Tatam, "Optical fibre long-period grating sensors: characteristics and application," *Measurement Science and Technology*, pp. R49-R61, 2003.
- [22] X. Shu, L. Zhang and I. Bennion, "Sensitivity characteristics of long-period fiber gratings," *Journal of Lightwave Technology*, vol. 20, no. 2, pp. 255-266, 2002.
- [23] R. Y. N. Wong, E. Chehura, S. E. J. S. Staines and R. P. Tatam, "Fabrication of fibre optic long period gratings operating at phase matching turning point using a UV laser," *Applied Optics*, vol. 53, pp. 4669-4674, 2014.
- [24] J. Cookney, W. Ogieglo, P. Hrabanek, I. Vankelecom, V. Fila and N. E. Benes, "Dynamic response of ultrathin highly dense ZIF-8," *Chemical communication*, vol. 50, pp. 11698--11700, 2014.
- [25] M. McCarthy, Varela-Guerrero, V., G. Barnett and H.-K. Jeong, "Synthesis of zeolitic imidazolate framework films and membranes with controlled microstructures," *Langmuir*, vol. 26, no. 18, pp. 14636-14641, 2010.

## Supporting information

### Organic vapour detection with use of optical fibre long period grating coated by ZIF-8 thin film

Jiri Hromadka<sup>1,2</sup>, Begum Tokay<sup>3</sup>, Sergiy Korposh<sup>1,4</sup> and Stephen James<sup>4</sup>

<sup>1</sup>*Applied Optics Group, Electrical Systems and Optics Research Division, Faculty of Engineering, University of Nottingham, University Park, Nottingham NG7 2RD, United Kingdom*

<sup>2</sup>*Institute for Environmental Studies, Faculty of Sciences, Charles University in Prague, Benátská 2, CZ 12843 Praha 2, Czech Republic*

<sup>3</sup>*Chemical and Environmental Engineering Department, Faculty of Engineering, University of Nottingham, University Park, Nottingham NG7 2RD, United Kingdom*

<sup>4</sup>*Department of Engineering Photonics, School of Engineering, Cranfield University, Cranfield, Bedfordshire MK43 0AL, United Kingdom*

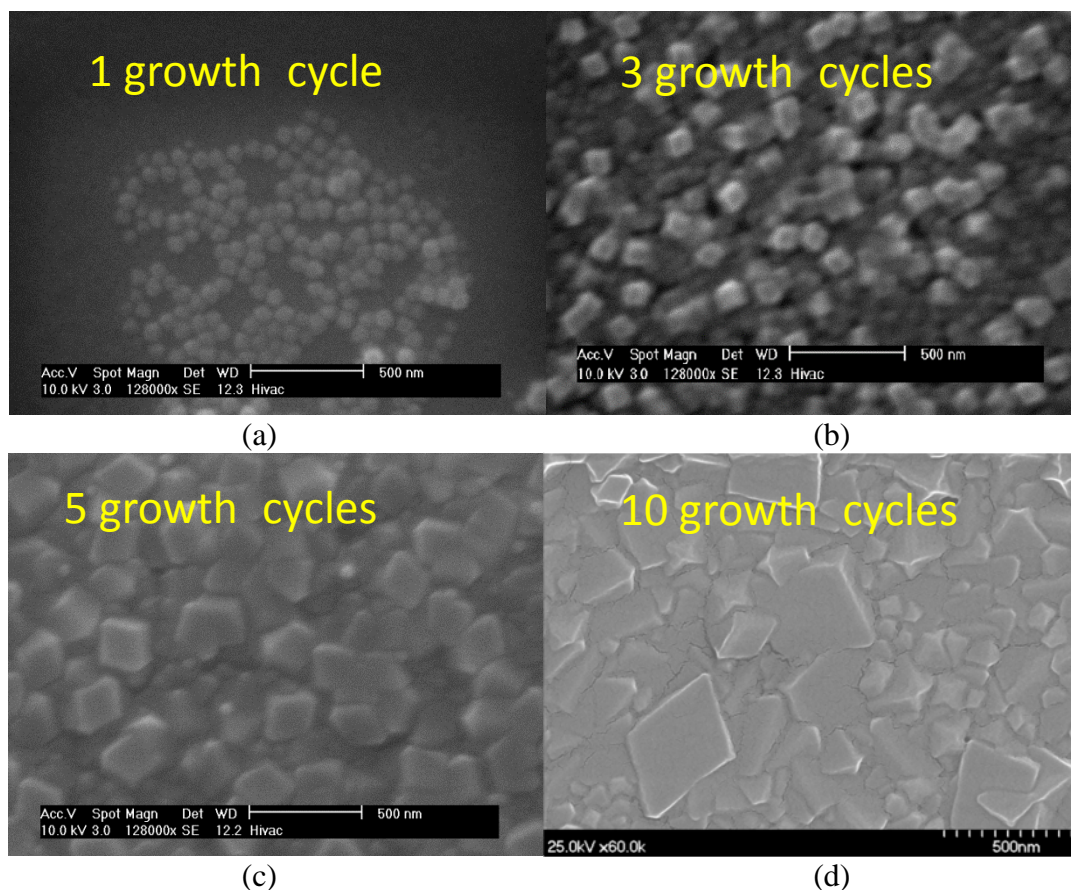


Figure S1: SEM images of ZIF-8 film comprised of a) one, b) three, c) five and d) ten growth cycles (the white at the bottom corresponds to 500 nm)

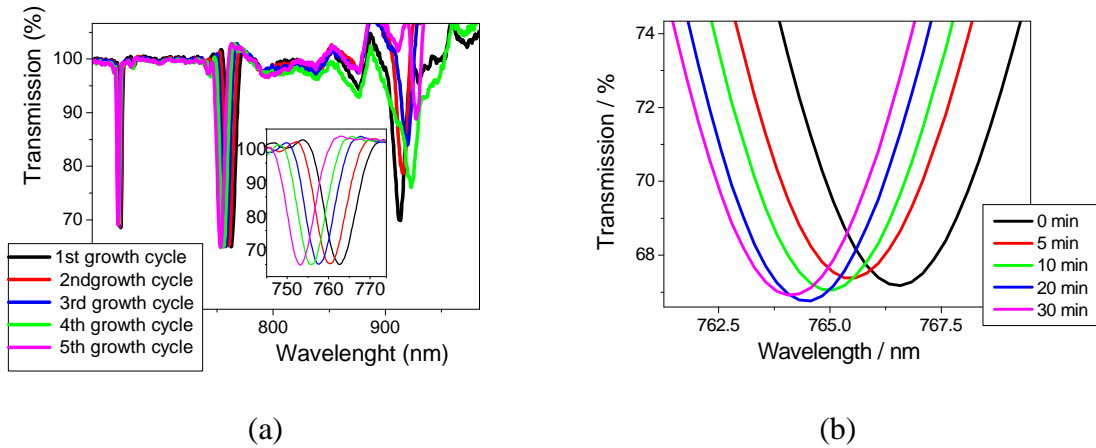


Figure S2: Transmission spectrum of LPG sensor measured in solution a) after 30 min of immersion to the film forming solution for 1<sup>st</sup> (black line), 2<sup>nd</sup> (red), 3<sup>rd</sup> (green), 4<sup>th</sup> (blue) and 5<sup>th</sup> (magenta) growth cycle of ZIF-8 and b) during the immersion and deposition of 1<sup>st</sup> growth cycle (black line shows the initial spectrum and red, green, blue and magenta lines shows the position of the attenuation band after the 5, 10, 20 and 30 min from the immersion).

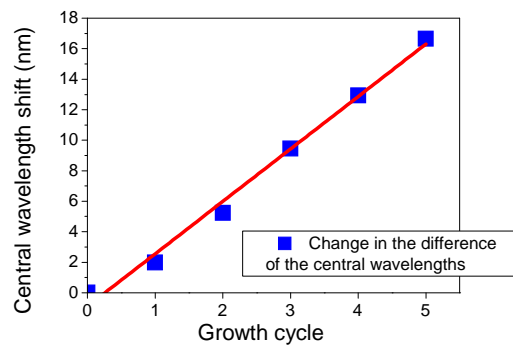


Figure S3: ZIF-8 deposition onto the surface of LPG with period of 110.7  $\mu\text{m}$ , central wavelength shift as a function of growth cycle

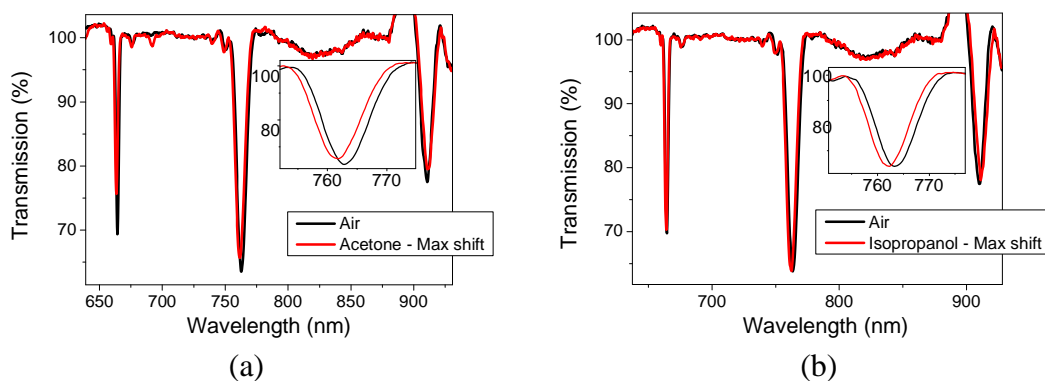


Figure S4: Transmission spectra of the LPG sensor with 5 growth cycles of ZIF-8 film exhibited to a) acetone and b) 2-propanol

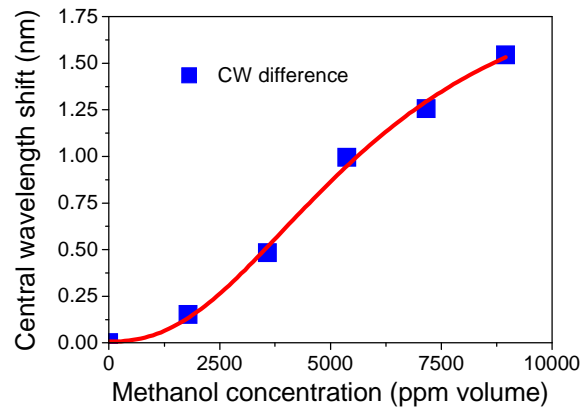


Figure S5: LPG sensor coated with 2 growth cycles of ZIF-8 - Methanol calibration curve